Green-state Micromilling of Additive Manufactured AISI316L

Sandeep Kuriakose [1]
Politecnico di Milano
Department of Mechanical Engineering, 20156, Milan, Italy
sandeep.kuriakose@polimi.it

Paolo Parenti
Politecnico di Milano
Department of Mechanical Engineering, 20156, Milan, Italy

Salvatore Cataldo
Politecnico di Milano
Department of Mechanical Engineering, 20156, Milan, Italy

Massimiliano Annoni
Politecnico di Milano
Department of Mechanical Engineering, 20156, Milan, Italy

ABSTRACT

Additive manufacturing (AM) of metal offers matchless design sovereignty to manufacture metallic micro components from a wide range of materials. Green-state micromilling is a promising method that can be integrated into the AM of metallic feedstock micro components in typical extrusion-based AM methods for compensating the inability to generate micro features. The integration enables the manufacturing of complex geometries, the generation of good surface quality and can provide exceptional flexibility to new product shapes. This work is a micromachinability study of AISI316L feedstock components produced by extrusion-based AM where the effects of workpiece temperature and the typical micromilling parameters such as cutting speed, feed per tooth, axial depth of cut and air supply are studied. Edge integrity and surface roughness of the machined slots, as well as cutting forces, are analyzed using 3D microscopy and piezoelectric force sensor, respectively. Green-state micromilling results were satisfying with good

[1] Corresponding author

produced quality. The micromilling of heated workpieces (45 °C), with external air supply for debris removal, showed the best surface quality with surface roughness values that reached around Sa = 1.5 µm, much smaller than the average metal particles size. Minimum tendency to borders breakage was showed but in some cases micro cutting was responsible of the generation of surface defects imputable to lack of adhesion of deposited layers. Despite this fact, the integrability of micromilling into extrusion-based AM cycles of metallic feedstock is confirmed.

Keywords: micromilling, extrusion, additive manufacturing, 3D printing, surface quality, feedstock.

1. INTRODUCTION

The extrusion-based methods for additive manufacturing (AM) of metallic components are increasing in popularity because of the recent advancements in the feedstock preparation, ease and low cost of production system, capability of producing parts with unique properties achievable by multiple materials and the small extent of material wasted during processing. The use of feedstock in the extrusion avoids the incapability of direct AM metal extrusion because of the problems due to the very high temperature, low viscosity and the surface tension of the molten metal [1]. The extrusion-based AM has strict connections with standard powder metallurgy process chains. The initial step consists in extrusion and deposition of metallic feedstock (i.e. a mixture of metallic powder and binder) micro filaments, layer by layer in the required geometry to produce a 3D part in green-state. This is followed by debinding of the part using solvent or thermal methodology to eliminate the binder and then sintering of the debound part to acquire the required final properties [2,3]. The final metal parts produced by extrusion-based AM could require finishing operations due to shrinkage, warpage and defects caused by debinding and sintering operations, but geometrical corrections of the part could also be very effective in the green-state because of the lower material hardness in the green-state than sintered state [4,5].

Micromilling can then be efficiently adopted on green-state material in order to compensate the geometrical inaccuracy of the material deposition, to increase surface finish, or to obtain microfeatures (such as microcavities and microchannels) which cannot be obtained with the deposition process [5]. For example, some internal surfaces could be milled before becoming inaccessible because of the following material deposition. As confirmed by previous micromilling studies by the authors [6] on hot-pressed AISI316L feedstock the green-state cutting force are extremely low. This fact increases the micro machinability and cost effectiveness of the cutting operations [7]. In that study, the integrity of the slot's top edge was influenced by cutting conditions and this proves how right parameters and their level selection is very significant for the successful integration of micromilling into the process chain [6]. By studying machinability of feedstock components produced by extrusion-based AM at green-state, this study extends what was done by the authors in previous studies. Effect of workpiece temperature on green machining is studied exclusively in addition to the micromilling parameters such as cutting speed (*vc*), feed per tooth (*fz*), axial depth of cut (*ap*) and air supply.

2. MATERIALS AND METHOD

2.1 Material

The feedstock material selected for experimental investigation is based on AISI316L. The metallic feedstock is produced in house with a percentage weight of 92.5 % of metal particles (D_{50} = 8.8 μm) compounded with water soluble polymeric binder (Embemould K83).

2.2 Additive manufactured workpiece preparation

Green-state workpieces used for the experimental investigation are feedstock blocks produced by AM using a prototype machine developed in house [8], Fig. 1. The blocks are printed in the preheated worktable by depositing continuous layers of extruded wires one above the other. The printing strategy consisted in *Infill* and *Shell* deposition as typical in FDM operation (see Fig. 2a and 2b).

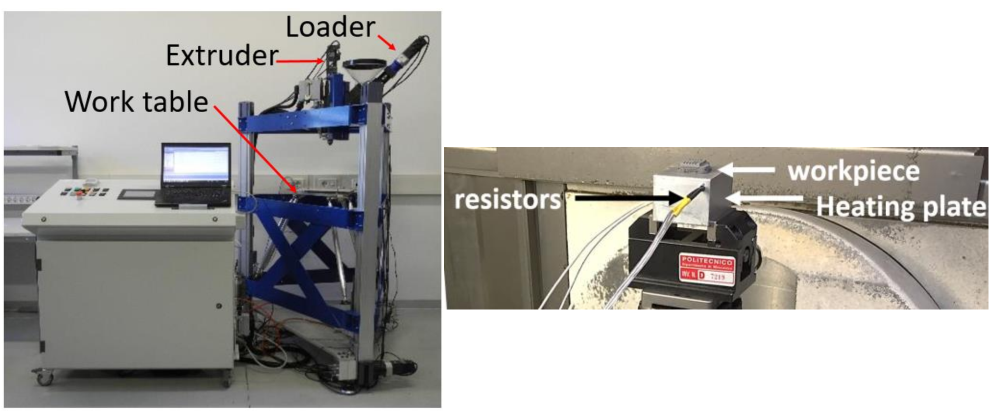

Fig. 1 Prototype extrusion AM machine and milling setup

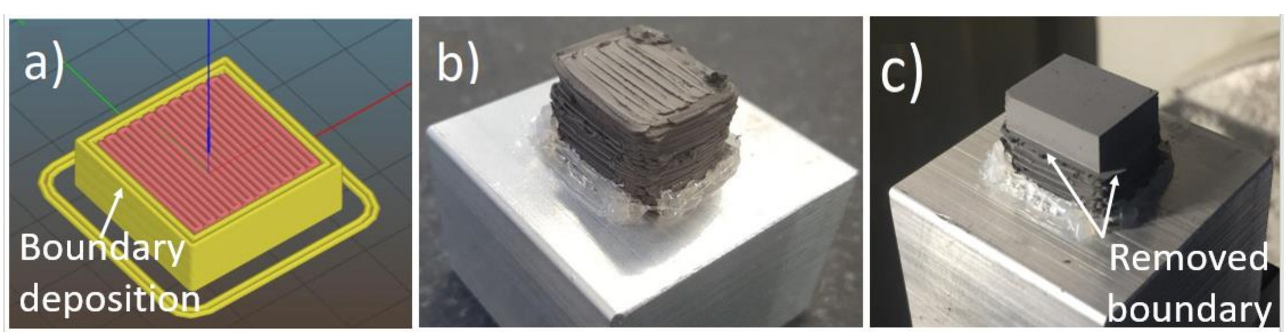

Fig. 2 Workpiece preparation a) Strategy used for AM, b) Workpiece produced by AM in green-state, c) AM workpiece after face milling and side milling operations

Then, the samples are prepared with standard face milling operations with a 6 mm tool, to generate smooth surfaces required for testing micromilling machinability. Bigger surface irregularities produced by the deposition process are then removed on the upper face and lateral faces (see Fig. 2c).

2.3 Experimentation

Micromilling experiments are conducted on three prepared green workpieces by milling micro slots of 1 mm in width and 5 mm in length by using a GF Mikron HPM 450U CNC machining center. Samples are fixed on a work base, attached to a triaxial piezoelectric dynamometer Kistler 9257B. Micro flat end mills, with tapered corners at 45°, 1 mm in diameter, PVD coated (AlCrN) and 2 teeth, are used for slot milling operations (Sandvik Coromant 1P220-0100-XA). A single tool is used for all experiments as no noticeable tool wear was observed in green-state micromilling of feedstock from previous studies [6]. Cooling air was used to refrigerate the cutting area and in addition a Vortex gun was used to refrigerate the air down to 5°C for testing the air temperature effect. A heated plate in aluminum with two resistors and one thermocouple, is used for controlling the temperature of the workpiece during both deposition and micromilling operations. The schematic diagram of milling setup is shown in Fig. 3. The experimentation is aimed at finding the factors that influence micromilling of the green samples produced by extrusion additive manufacturing by the prototype machine.

Micromilled slots are then analyzed for edge integrity and surface roughness using 3D microscopy (Alicona G4) and optical profilometry (Mitutoyo Quick Vision Pro) and acquired cutting force signals are analyzed for each micromilling condition in Matlab and Minitab. The cutting forces are acquired at 25 kHz and depurated from the sensor pure dynamic response. Resultant force Fr is computed from forces in X-Y-Z and RMS value over the contact time is analyzed.

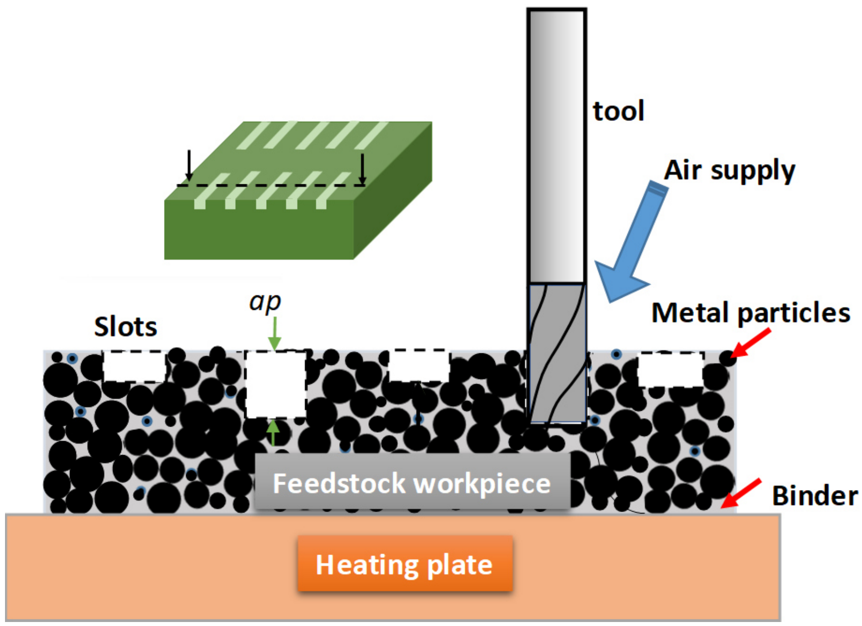

Fig. 3 Schematic diagram of feedstock micromilling

The average surface height, Sa, was used as indicator for quantitative roughness analysis. The samples in each set of experiments are also analyzed using scanning electron microscope (SEM) to understand in depth the changes during debinding, pre-sintering and sintering operations.

Experiments are conducted in six sets, Table 1. The experiments from set 1 to 5 are conducted, consequently, on workpieces 1 and 2 (WP1 and WP2 in Table 1) by alternating milling and measurements of the slots followed by a flattening operation to re-establish a clean surface for the next testing. In the case of set 3, a part of experiments is conducted on WP1 and other part on WP2. The third workpiece, (WP3 in Table 1) is solely used for understanding the effect of debinding and sintering on the micromilled extrusion additive manufactured samples.

Table 1: Experiments summary

Set	Variable	Levels		Constant parameter
1 (WP1)	*vc*	17.5	35	*fz*=0.03, T_{air}=22.5, T_{WP}=22.5
	ap	0.25	0.5	
2 (WP2)	*fz*	0.015	0.03	*ap*=0.5, *vc*= 35, T_{WP}=22.5
	T_{air}	Air off	5	
3 (WP1-2)	*vc*	17.5	35	*ap*=0.5, T_{WP}=45
	fz	0.015	0.03	
	T_{air}	Off	22.5	
4 (WP1)	*fz*	0.02-0.03-0.04-0.05		*ap*=0.5, *vc*=26.25,T_{air}=22.5,T_{WP}=45
5 (WP2)	*fz*	0.02-0.03-0.04-0.05		*ap*=0.5, *vc*=26.25, T_{air}=22.5, T_{WP}=22.5
6 (WP3)	Nil	-	-	*ap*=0.5 x 2 passes (total depth =1mm), *vc*=35, *fz*=0.03, T_{air}=22.5,T_{WP}=22.5

vc [m/min], *ap* [mm], *fz* [mm/tooth], T_{air} and T_{WP} [°C]

The micromilling parameters range is selected basing on some screening tests on deposited samples and previous experience of authors on AISI316L feedstock [6]. The gap between adjacent slots are twice the slot width to avoid any unwanted neighboring effect. One pass is prescribed per slot producing a slot depth equal to the adopted axial depth of cut.

In the first two sets of experiments in Table 1, the study of the influence of milling parameters such as *vc, fz* and *ap* and the effect of the refrigerated air supply (temperature of air, T_{air} = 5 °C) is carried out. The experiment sets 3 and 4 are conducted by maintaining the workpiece (workpiece temperature, T_{WP} = 45 °C) in heated stage (in order to mimic the temperature of the workpiece right after the AM). The study is expected to provide the essential information required for integrating micromilling to the extrusion-based AM process chain. Air flow is provided from a suitable distance not to disturb the heating plate effect and, at the same time, assuring the debris removal. Experiments are conducted in three repetitions in randomized order. The fifth experiment is used to compare how material specific cutting energy changes with respect to workpiece temperature, and it is directly comparable with test number four. The sixth set is conducted by cutting 12 slots in workpiece 3 and then debinding the sample using water at 40 °C followed by thermal debinding in H_2 atmosphere and finally pre-sintering at 680 °C. This sample is then sintered in 3 % argon tube furnace at a temperature of 1340 °C.

RESULTS AND DISCUSSION

3.1 Force analysis

The influence of the tested cutting parameters (set 1 and 2 in Table 1) during machining operations are analyzed in terms of main and interaction effects (Fig. 4). The RMS values of the resultant forces remain below 2.5 N. From the statistical perspective, the only *ap* and *fz* parameters show direct effect (p-value < 0.05) on the force: doubling these values produces an increase of almost 40 % of the force value. On the other side, the air and *vc* and their interactions did not affect forces significantly. The *ap* affects chip section and doubling it implies doubling the chip nominal area formed during cutting. An increase of only 40 % suggests that it is relatively easy to cut longer chip section than shorter and this may be probably due to the effects of ploughing on the binder component of the material as the chip area is big. The reasons why resultant forces were not affected by air and *vc* are not exactly clear. On one side, increasing *vc* affects the heat generation and the cutting temperature obtained, introducing some thermal softening into the material (due to binder components) and that could reduce forces. Probably this lowering effect on the forces is negligible or it is zeroed by an increase in the cutting energy due to other intrinsic effects due to the special material properties. Further investigation and advanced process modelling are required to clarify this. At the same time, the air helped in avoiding chip remachining and kept the area clean from debris, and introduced some temperature reduction effect (due to air convection). The fact that air did not affect forces significantly could be still related with a reduced effect of cutting temperature on the force generation, according to what happened with the *vc*. This shows how green components machining generates lower forces, an order of magnitude smaller than that of values of sintered material. There are no evident outliers as well. Interaction analysis shows no statistical evidence of interactions (p-value > 0.05) between the varying parameters.

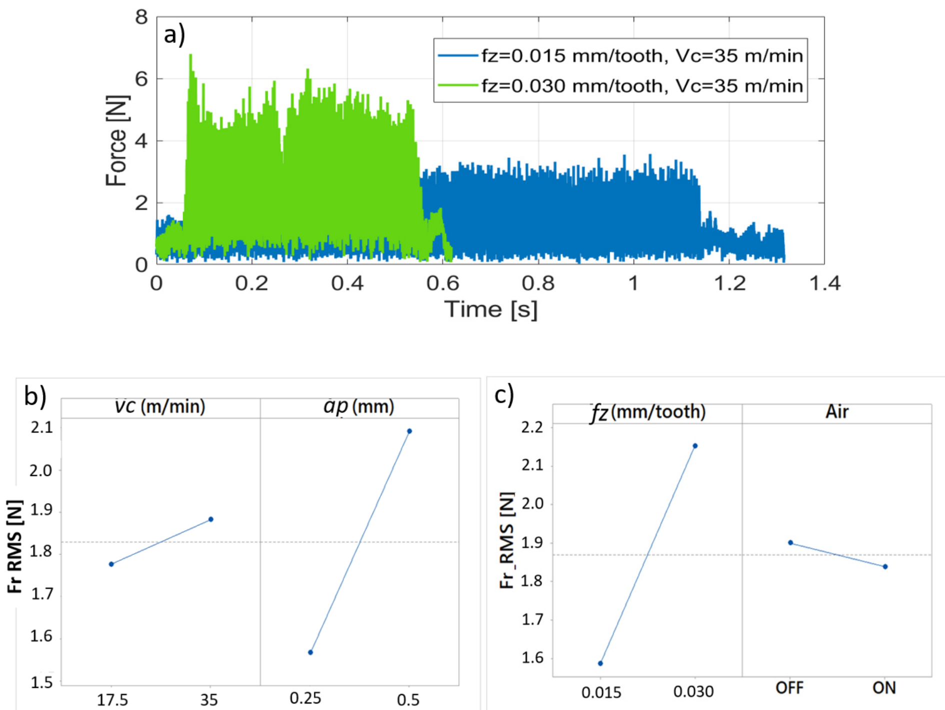

Fig. 4 (a) Cutting force signals set 2 (T_{air} = 5, T_{WP} = 22.5, ap = 0.5), (b)-(c) Main effect plots set 1 and set 2.

Variation of the cutting forces with the workpiece temperature (set 4 and 5 in table 1) is tested by heating up the sample to T_{WP}= 45 °C and testing the force variability in respect to ambient temperature (T_{air} = 22.5 °C). Heated conditions of the workpiece generate more force variability within the replicas and stronger sensitivity of the forces to the feed, Fig.5. Bigger forces in heated condition are found but however, force magnitude difference is low, around 20 % in RMS value. This increase could be linked to the increased friction and adhesion tendency of the heated workpiece material during cutting.

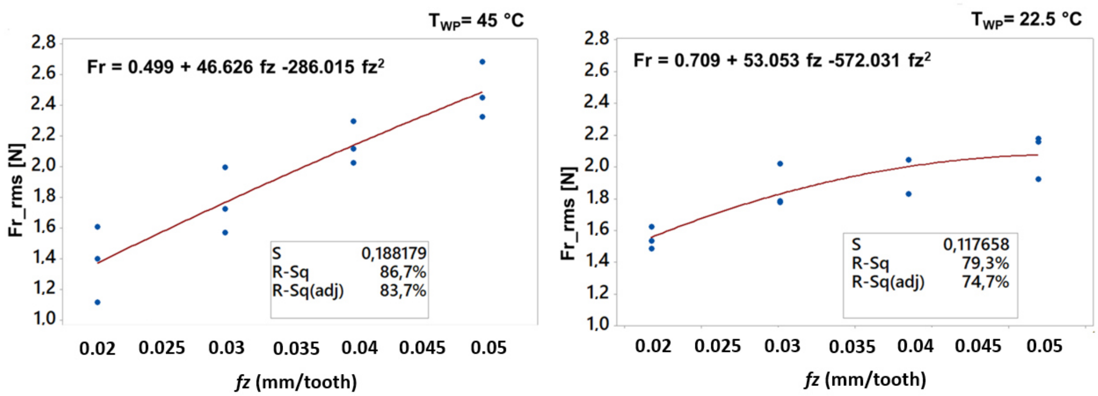

Fig. 5 RMS force value during heated and cold workpiece condition, set 4 (left) and 5 (right)

3.2 Surface quality

Micromilling of workpieces produced by extrusion additive manufacturing showed a good machinability and thereby generally a good surface and edge quality. However, some macro defects such as large border breakage happens rarely in some cases. The reason for this large border breakage (Fig. 6) is attributed mainly to the lack of adhesion between the adjacent layers during extrusion additive manufacturing. In any case micromachining triggered this large border breakage to happen and thereby has an effect somehow. Optimizing the AM parameters may help to avoid this problem.

3.2.1 Surface quality of green samples

The roughness analysis of the milling experiment on workpieces at 22.5 °C temperature (set 1 in Table 1) gives a maximum Sa value of 2.85 µm and minimum value of 1.46 µm, while experiments in set 2 gives a maximum and minimum values of 2.93

µm and 2.15 µm respectively, which are unexpectedly good values for the green-state material (Fig 6).

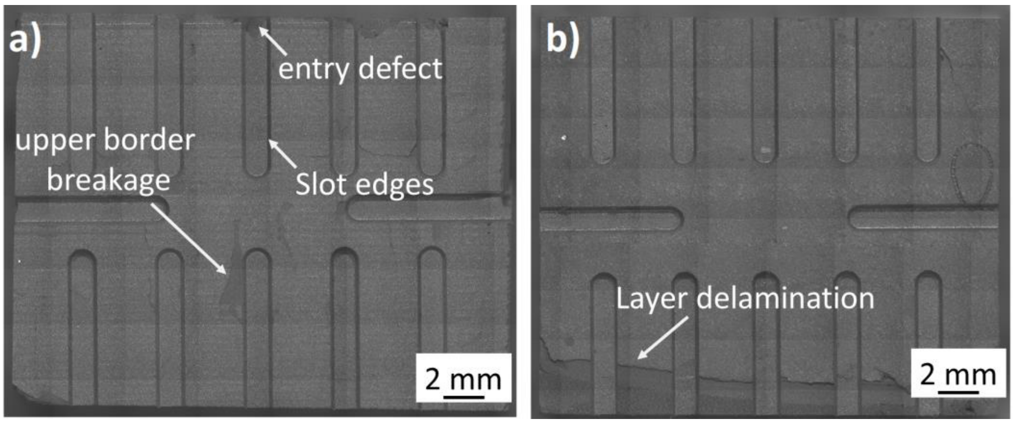

Fig. 6 Optical microscope images of exp. a) set 1 and b) set 2

However, the roughness values in both sets 1 and 2 vary only marginally with a variation of the different factors. Main effect plot showed only a minor influence of *fz, ap* and refrigerated air supply temperature, except *vc*. The interaction plot denied the possible interaction between the factors. ANOVA and verification of the assumptions showed that there are neither significant factors nor interactions which influence the surface roughness for the selected ranges and levels (p-value < 0.05).

An analysis with wide spread levels may need to be performed to understand the significance of parameter variations in case of green-state micromilling of AM workpiece at room temperature. The micromilling of the first stage of exp. set 3, without an air supply for chip removal resulted in material remachining and difficult debris evacuation from the cutting zone. Top burr formation, augmented border breakages, and debris attachments to the slot boundary (Fig. 7a) are evidenced after cutting. This is probably caused by the increased adhesion effect of the polymeric binder at the higher temperature. The milling experiments in the second stage of exp. set 3 are conducted with a supply of pressurized air at ambient temperature from a far distance (300 mm) in order to increase the debris removal. This condition resulted in a good surface finish (Fig. 7b) and reduced the overall defects.

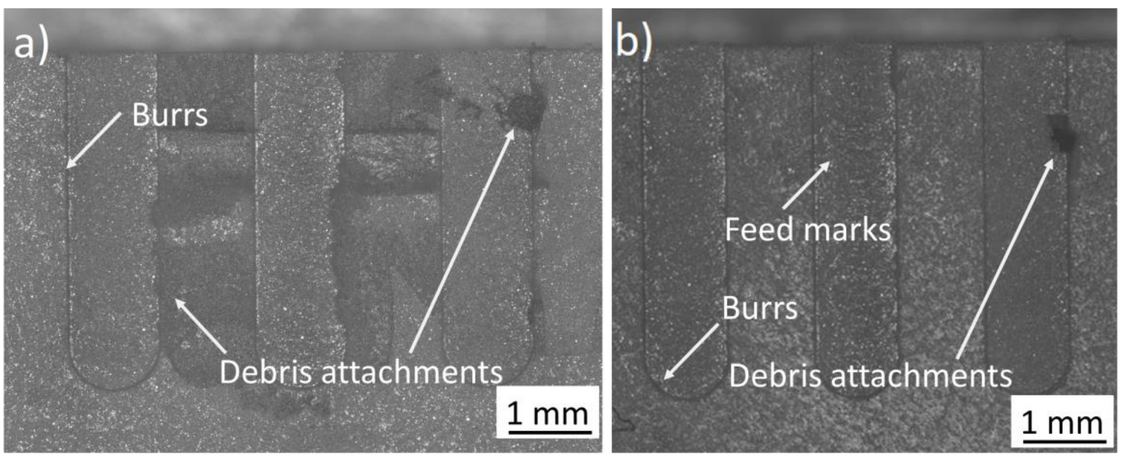

Fig. 7 Optical microscopic analysis on set 3 a) exp. without air supply and b) exp. with air supply

Roughness is measured at start, middle and end positions along the slots (Fig. 8). The main effect plot shows that roughness values are lower for the lower levels of *vc* and *fz.* The roughness value does not change significantly along the slots. *fz* seemed to be the most significant factor with p-value < 0.05. *vc* and slot positions did not show to be significant with p-value > 0.05.

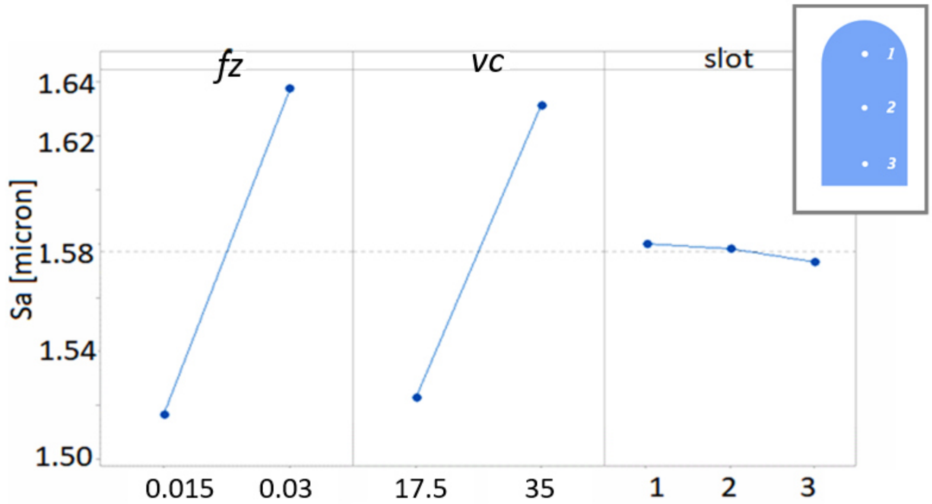

Fig. 8 Main effect plot of Sa surface roughness: (*fz, vc* and slot measured position)

The roughness analysis of the micromilling experiments with the workpiece at cold (22.5 °C) and heated (hot) state (45 °C) from comparison of the corresponding conditions of set 6 (green-state) and set 3 showed a decrease in Sa value with respect to an increase of workpiece temperature (Fig. 9). This result is probably due to the softening of the binder content at high temperature, which could have supported the generation of a better surface quality. This aspect will receive attention in further studies.

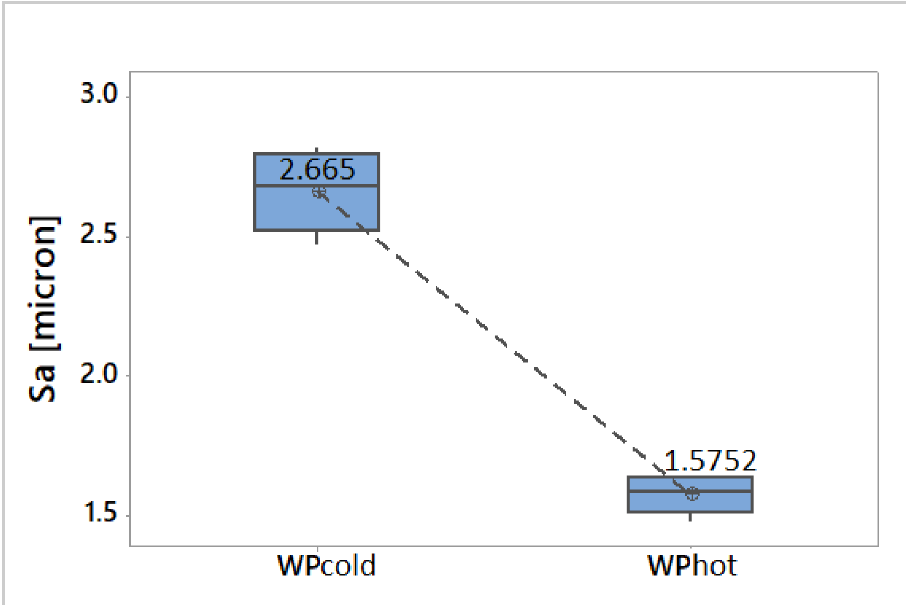

Fig. 9 Box plots comparison of roughness analysis for milling exp. on workpiece at hot (45 °C) and cold (22.5°C) state

3.2.2 Surface quality of green, brown and sintered samples

The brown and sintered workpiece surfaces showed nice surface quality without any cracks or air entrapment defects (Fig. 10). The sintering operation causes the diffusion of atoms and forms bonds between the metal particles by reducing the porosity inside the material. The roughness analysis of the green, brown and sintered samples showed gradual increase in the mean value of roughness (Fig. 11). The increase of roughness is caused by the binder removal by debinding and pre-sintering and consequent variation of surface asperities. Generation of micro superficial voids however seemed not to play a big role on the overall roughness in terms of Sa values.

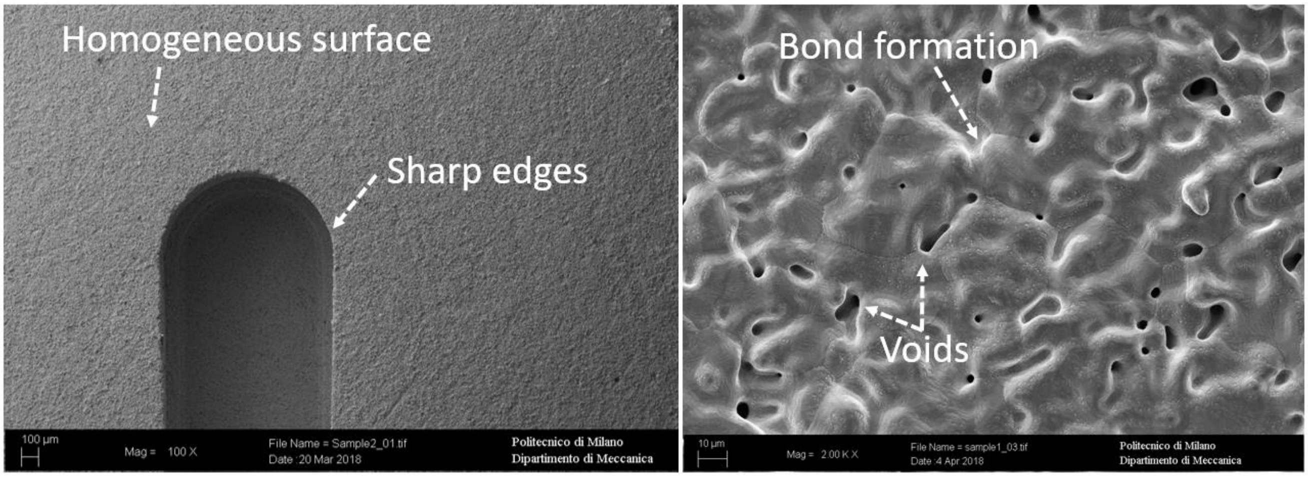

Fig. 10 The SEM image of the workpiece in brown state (left), and micro structure showing porosity reduction by sintering (right)

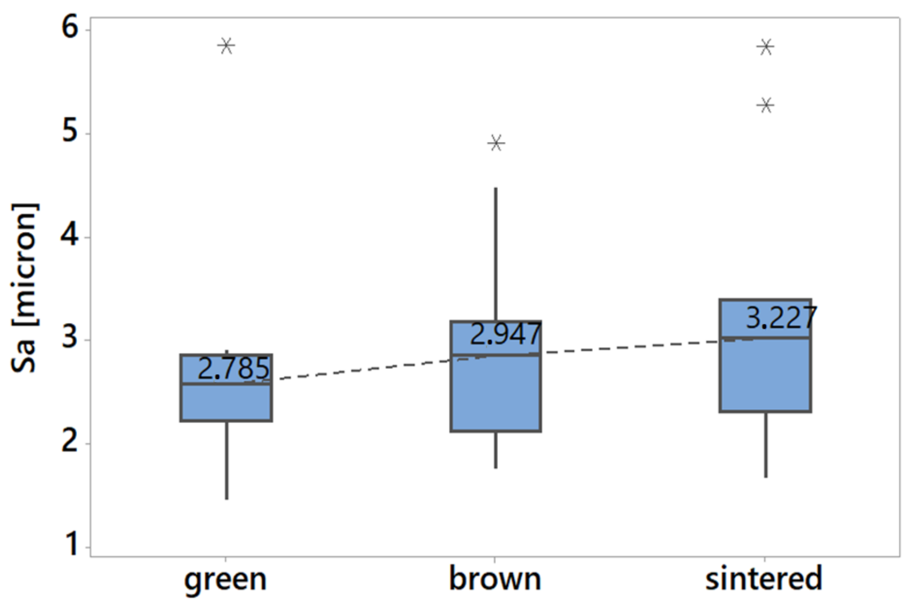

Fig. 11 Box plot comparison of roughness analysis for green, brown and sintered states

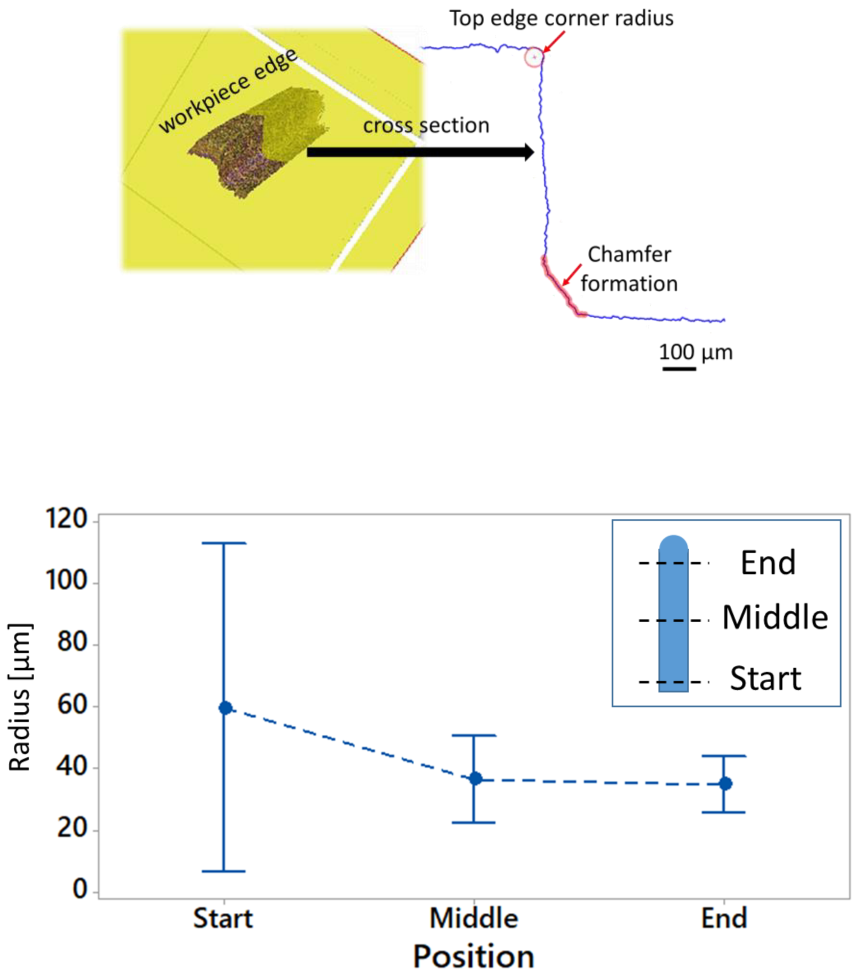

Fig. 12 Corner radius measurement of the top edges of the slots (sintered)

Integrity of the corners is also studied. It was decided to measure the corner radius of the top corner to see what are the achievable radii in the sintered sample. The analysis of set 6 (Table 1) showed an average corner radius value of 43 µm. In case of bottom edge, a chamfer formation was observed according to mill geometry. The average corner radius of 59 µm, 36 µm and 34 µm were observed for sintered sample for start, middle and end positions of the slots respectively (Fig. 12). However, a higher variation was observed for start position of the edge, already from green-state, probably due to the adoption of multiple (two) passes to reach the overall slot depth of 1 mm.

3.3 Defects and specific features on surfaces produced by micromilling

Micromilling experiments on green feedstock workpieces produced by extrusion AM generally milled slots with good edge integrity and surface quality. Some of the defects observed are breakage of the edges, chamfer formation from the shape of milling cutter, and burr attachment to the edges of the milled slots (Fig. 13).

The micromilling operations seemed to produce breakage of the slot edges. The soft nature of the feedstock in green-state accounts for this problem. Feedstock with an increased binder percentage may able to solve this defect by improving the adhesion between the metal particles.

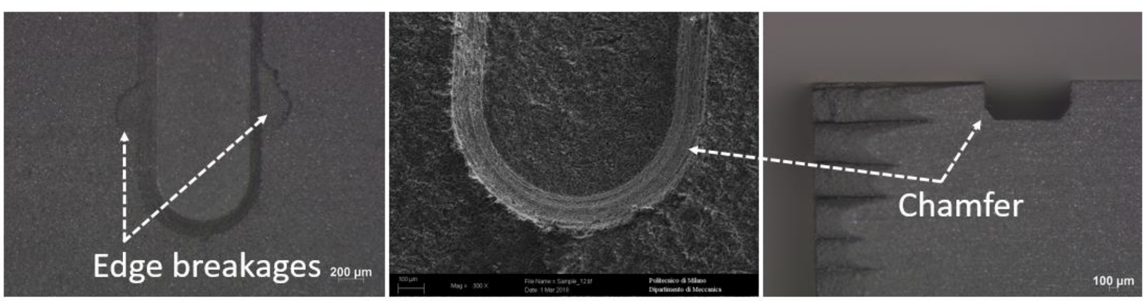

Fig. 13 SEM Image of breakage of the slot edges (first), chamfer formation from the shape of milling cutter (second) and cross-sectional view showing chamfer formation (third)

The layers formed by AM and surface after side milling also can be observed and compared from the cross-sectional view. The side milled surface did not show any porosity, which means that successive layers in AM was fused together in a better manner.

It is possible to observe, Fig. 13, that the slot depth is equal to layer thickness. Despite that micromilling process could in most of the cases obtain good cuts without layer delamination indicating good interlayer adhesion.

4. CONCLUSIONS

Force analysis confirmed that generated forces during green-state micromilling of extrusion additive manufactured parts is very low, comparable to hot pressed feedstock and more than an order of magnitude lower than sintered material. Milling parameters *ap* and *fz* showed to be the significant parameters on the force in a directly proportional way. Lower levels of *ap* and *fz* values are observed to be suitable for low force generation.

Micromilling of heated workpieces with an air supply for chip removal purposes showed the best surface quality with the least surface roughness. *fz* seemed to be the most significant milling parameter and the lower values of *fz* and *vc* are found to be apt for the green-state micromilling.

This preliminary study on extrusion based additive manufactured material clarifies how micromilling is a suitable post-processing method that can be implemented in standard AM of green components. Future studies will be devoted to hybrid in-line testing of the micromilling process in the extrusion-based AM approaches.

ACKNOWLEDGMENTS

The authors are grateful to Marco Covelli, Alberto Grigis (Politecnico di Milano), G. De Gaudenzi F.I.L.M.S. Spa and Valerio Mussi (MUSP) for their support.

FUNDING

This research work was undertaken in the context of MICROMAN project ("Process Fingerprint for Zerodefect Net-shape MICROMANufacturing", http://www.microman.mek.dtu.dk/). MICROMAN is a European Training Network supported by Horizon 2020, the EU Framework Programme for Research and Innovation (Project ID: 674801).

REFERENCES

[1] Joamin, G., Santiago, C., Stephan, S., Christian, K., Janak, S., and Clemens, H., 2018. "Additive Manufacturing of Metallic and Ceramic Components by the Material Extrusion of Highly-Filled Polymers: A Review and Future Perspectives." Materials 11:840

[2] Cristofolini, I., Rao, A., Menapace, C., and Molinari, A., 2010, "Influence of Sintering Temperature on the Shrinkage and Geometrical Characteristics of Steel Parts Produced by Powder Metallurgy," J. Mater. Process. Tech., 210(13), pp. 1716–1725.

[3] Attia, U. M., and Alcock, J. R., 2011, "A Review of Micro-Powder Injection Moulding as a Microfabrication Technique," J. Micromechanics Microengineering, 21(4), pp. 1–22.

[4] Dadhich, P., Srivas, P. K., Mohanty, S., and Dhara, S., 2015, "Microfabrication of Green Ceramics: Contact vs. Non-Contact Machining," J. Eur. Ceram. Soc., 35(14), pp. 3909–3916.

[5] Parenti, P., Cataldo, S., and Annoni, M., 2018, "Shape Deposition Manufacturing of 316L Parts via Feedstock Extrusion and Green-State Milling," Manuf. Lett., 18, pp. 6–11.

[6] Parenti, P., Kuriakose, S., and Annoni, M., 2017, "Green-state micromilling of AISI316L feedstock", Proceedings of the World Congress of Micro and Nano Manufacturing WCMNM 2017, Taiwan, 2017

[7] Bukvic, G., Sanchez, L. E. D. A., Fortulan, C. A., Fiocchi, A. A., and Marinescu, I. D., 2012, "Green Machining Oriented to Diminish Density Gradient for Minimization of Distortion in Advanced Ceramics," Mach. Sci. Technol., 16, pp. 228–246

[8] Annoni, M., Giberti, H., and Strano, M., 2016, "Feasibility Study of an Extrusion-Based Direct Metal Additive Manufacturing Technique," Procedia Manuf., 5, pp. 916–927.